



# Influence of the nature and environment of vanadium in VSiBEA zeolite on selective catalytic reduction of NO with ammonia

Rafal Baran<sup>a,c</sup>, Thomas Onfroy<sup>a,b</sup>, Teresa Grzybek<sup>c</sup>, Stanislaw Dzwigaj<sup>a,b,\*</sup>

<sup>a</sup> UPMC Univ Paris 06, Laboratoire de Réactivité de Surface, Case 178, Site d'Ivry-Le Raphaël, 3 rue Galilée, 94200 Ivry sur Seine, France

<sup>b</sup> CNRS-UMR 7197, Laboratoire de Réactivité de Surface, Case 178, Site d'Ivry-Le Raphaël, 3 rue Galilée, 94200 Ivry sur Seine, France

<sup>c</sup> AGH University of Science and Technology, Faculty of Energy and Fuels, Al. A. Mickiewicza 30, 30-059 Krakow, Poland



## ARTICLE INFO

### Article history:

Received 2 December 2012

Received in revised form 29 January 2013

Accepted 1 February 2013

Available online 16 February 2013

### Keywords:

Vanadium

Ammonia

NO

BEA

FTIR

DR UV–vis

TPR

SCR

## ABSTRACT

The influence of the nature and environment of vanadium on the catalytic properties of V<sub>x</sub>SiBEA zeolite in selective catalytic reduction of NO with ammonia is investigated. Catalysts containing 1–7.5 wt.% of vanadium were prepared by a two-step postsynthesis method which consists, in the first step, of dealumination of TEABEA zeolite to obtain SiBEA support and then, in the second step, of contacting the obtained material with an aqueous solution of NH<sub>4</sub>VO<sub>3</sub> at pH 2.7. XRD and low temperature N<sub>2</sub> sorption results show that full dealumination of parent TEABEA zeolite by nitric acid treatment as well as incorporation of vanadium atoms in the framework of SiBEA zeolite do not change the crystallinity of BEA zeolite. The presence of isolated pseudo-tetrahedral V(V) species for low V content and pseudo-tetrahedral and octahedral V(V) species for high V content is evidenced by diffuse reflectance UV–vis, Raman and TPR. The catalytic activity of V<sub>x</sub>SiBEA in selective catalytic reduction of nitric oxide with ammonia as reducing agent strongly depends on the nature and environment of vanadium in BEA structure. The single site V<sub>1.0</sub>SiBEA catalyst with isolated pseudo-tetrahedral V(V) species is active in SCR of NO process, with maximum NO conversion about 60% at 773 K and with very low selectivity toward undesired N<sub>2</sub>O. In contrast, V<sub>3.0</sub>SiBEA and, especially, V<sub>7.5</sub>SiBEA catalyst containing mainly extra-framework octahedral V(V) and vanadium oxide species are less active in SCR of NO process at higher temperature and big amount of N<sub>2</sub>O is observed in the product stream.

© 2013 Elsevier B.V. All rights reserved.

## 1. Introduction

The selective catalytic reduction of NO<sub>x</sub> over vanadia/titania catalysts with WO<sub>3</sub> or MoO<sub>3</sub> promoters is the most common and efficient method for nitric oxides abatement. These catalysts, widely applied at 573–673 K temperature range, are characterized by high activity and good selectivity to N<sub>2</sub> [1–3].

However, to remove NO<sub>x</sub> from outgases at high temperature (673–773 K) it is necessary to use other type of catalysts which are more stable as well as have strong chemical resistivity to poisoning substances such as SO<sub>x</sub> or alkaline metals. Zeolites, especially those with high Si/Al ratio and wide pore structure allowing easy diffusion of reaction substrates and products without mass transport limitation seem to be promising materials [4,5].

Furthermore, zeolites should contain active sites as well dispersed transition metal species, because the formation of metal oxides clusters leads to low selectivity to desired products in SCR

reaction and they are less stable at high temperatures resulting in sharp decrease in NO conversion [6–8].

Since 1986, when Iwamoto et al. discovered the remarkable activity of Cu-ZSM-5 catalyst in NO removal, a lot of work has been done to understand the role of transition metal ions exchanged in zeolites in catalytic reduction of NO<sub>x</sub>, as well as to optimize the procedure of catalysts preparation [6,9,10]. Moreover, one of the major challenges in this process is to understand its mechanism and the role of different metal species in the elimination of nitric oxides. Another important problem is finding the reason for N<sub>2</sub>O formation during the process of SCR of NO with ammonia. Up to now different mechanisms have been considered for N<sub>2</sub>O formation [11–16].

Recently [17–20], vanadium containing zeolites have been investigated in reduction of nitric oxides. Putluru et al. [17] have been used several types of vanadium doped zeolites, such as HBETA, HY, HZSM5 containing different amount of vanadium (3–16 wt.%). They have found that NO conversion was strongly influenced not only by metal content but also by Si/Al ratio. A similar conclusion has been proposed by Piehl et al. indicating that acidity improved activity in selective catalytic reduction of NO with ammonia [21].

Several types of vanadium species can be present on the vanadium containing zeolite catalysts surface at reaction conditions, each with specific catalytic properties: isolated mononuclear,

\* Corresponding author at: UPMC Univ Paris 06, Laboratoire de Réactivité de Surface, Case 178, Site d'Ivry-Le Raphaël, 3 rue Galilée, 94200 Ivry sur Seine, France. Fax: +33 1 44 27 21 13.

E-mail address: [stanislaw.dzwigaj@upmc.fr](mailto:stanislaw.dzwigaj@upmc.fr) (S. Dzwigaj).

polynuclear with bridging oxygen, vanadium hydroxyl, vanadium center with oxygen vacancies. The preferred form of vanadium on titania catalysts is rather mononuclear than bulk vanadium pentoxide because of poor selectivity to  $\text{N}_2$  of large aggregates of  $\text{VO}_x$  [22–24]. On the other hand, it has been reported that at low reaction temperature (573 K) the polynuclear vanadium species are more active in SCR of NO with ammonia than mononuclear ones [25,26]. So, it is still not clear which kind of vanadium center is more active in SCR of NO process.

In this work,  $\text{V}_x\text{SiBEA}$  zeolites are prepared by two-steps post-synthesis method which allows to control their preparation and to obtain catalysts with isolated mononuclear vanadium species incorporated into zeolite framework for low V content (<2 wt.%) [27] and  $\text{V}_x\text{SiBEA}$  zeolites possessing besides mononuclear framework V also polynuclear V species in extra-framework position for much higher V content (>3 wt.%). Prepared material with low V content is unique because of the high level of metal dispersion and pseudo-tetrahedral coordination of vanadium species, as well as its high thermal stability.

The subject of this work is investigation of the influence of the nature and environment of vanadium species present in  $\text{VSiBEA}$  zeolite on selective catalytic reduction of NO with ammonia as reducing agent.

## 2. Experimental

### 2.1. Catalyst preparation

A tetraethylammonium BEA (TEABEA) zeolite with atomic Si/Al ratio of 17 provided by RIPP (China) was dealuminated by a treatment with nitric acid solution ( $c = 13 \text{ mol dm}^{-3}$ ) at 353 K for 4 h, to obtain dealuminated SiBEA with atomic Si/Al ratio of 1141 and then washed several times with distilled water and dried at 368 K overnight. Then, obtained material was contacted with an aqueous  $\text{NH}_4\text{VO}_3$  solution in excess (2 g of zeolite in 200 ml of solution) at pH 2.7 and stirred for 24 h at 298 K. A concentration of  $\text{NH}_4\text{VO}_3$  solution was varied from  $1.96 \times 10^{-3}$  to  $1.47 \times 10^{-2} \text{ mol L}^{-1}$ . At pH 2.7 and because of its low concentration, the aqueous  $\text{NH}_4\text{VO}_3$  solution is expected to contain mainly mononuclear  $\text{VO}_2^+$  ions [28]. Then, the suspensions were stirred in evaporator under vacuum of a water pump for 2 h in air at 333 K until the water was completely evaporated. As obtained vanadium containing samples were labeled  $\text{V}_x\text{SiBEA}$  with  $x = 1\text{--}7.5 \text{ wt.}\%$ .

### 2.2. Catalyst characterization

X-ray Fluorescence chemical analysis was performed at room temperature on SPECTRO X-LabPro apparatus.

XRD profiles were recorded at room temperature on a PANalytical Empyrean diffractometer using the  $\text{CuK}\alpha$  radiation ( $\lambda = 154.05 \text{ pm}$ ).

Specific surface area and adsorption isotherms of nitrogen at 77 K were measured on a Micromeritics ASAP 2010 apparatus. All samples were outgassed, first at room temperature, then at 623 K to a pressure <0.2 Pa. The specific surface areas were determined from nitrogen adsorption values from  $P/P^0 = 0.05\text{--}0.16$  using BET method. The microporous pore volume was determined from the amount of  $\text{N}_2$  adsorbed up to  $P/P^0 = 0.2$ .

FTIR spectra were recorded on Bruker Vector 22 spectrometer equipped with DTGS detector with a  $2 \text{ cm}^{-1}$  resolution and a number of scan of 128. Samples were pressed at  $0.5 \text{ tons cm}^{-2}$  into thin wafers of about  $10 \text{ mg cm}^{-2}$  and placed inside the IR cell. The wafers were calcined in static conditions at 723 K for 3 h in presence of  $\text{O}_2$  ( $1.6 \times 10^4 \text{ Pa}$ ) and then outgassed under secondary vacuum

( $10^{-3} \text{ Pa}$ ) at 573 K for 1 h. After that, the wafers were cooled down to room temperature and the spectra were recorded.

The mixture of KBr and zeolite sample (200:1) was carefully ground and pressed into a wafer under pressure of  $2 \text{ tons cm}^{-2}$ . The framework vibrational spectra were recorded between 400 and  $1300 \text{ cm}^{-1}$  with a resolution of  $4 \text{ cm}^{-1}$ .

DR UV–vis spectra were recorded at ambient atmosphere on a Cary 5000 Varian spectrometer equipped with a double integrator with polytetrafluoroethylene as reference.

Raman spectra were recorded in the  $100\text{--}3450 \text{ cm}^{-1}$  range on a spectrometer (Model HL5R Kaiser Optical Systems, Inc.) connected to a microscope (Olympus, objective:  $100\times$ ). It is equipped with a high-powered near-IR laser diode working at 785 nm. The optical microscope was used to focus the laser beam. Each analysis was the result of 10 acquisitions of 30 s at 20 mW.

EPR spectra were recorded on a JEOL FA-300 series EPR spectrometer at  $\approx 9.3 \text{ GHz}$  (X band) using a 100 kHz field modulation and a 5 Gauss standard modulation width. The spectra were recorded at 77 K.

The  $\text{H}_2$ -TPR measurements were carried out on an AutoChem 2910 apparatus (Micromeritics) in the temperature range 298–1173 K with a linear heating rate of  $7 \text{ K min}^{-1}$ . 0.1 g of sample was reduced in hydrogen stream (5%  $\text{H}_2/\text{Ar}$ ) with a gas volume velocity of  $0.04 \text{ L min}^{-1}$ . Hydrogen consumption was monitored with a thermal conductivity detector (TCD). Before experiments,  $\text{V}_x\text{SiBEA}$  were calcined at 773 K for 3 h in static conditions and then rehydrated by exposure to moist air.

### 2.3. Catalysts activity measurements

The activity of  $\text{V}_x\text{SiBEA}$  catalysts in selective catalytic reduction (SCR) of NO with ammonia was measured in a conventional fixed-bed reactor. Temperature was measured inside the reactor with a thermocouple and controlled with an electronic controller (LUMEL RE19). The composition of reaction mixture was: 1000 ppm NO, 1000 ppm  $\text{NH}_3$ , 3.5 vol.%  $\text{O}_2$  and He as balance. The gas mixture was fed using calibrated electronic mass flow controllers (BETA-ERG). The total gas flow was  $0.1 \text{ L min}^{-1}$  and catalyst mass was 0.2 g. The concentration of NO and  $\text{N}_2\text{O}$  were analyzed by FTIR detectors (ABB 2000 AO series). Before the catalytic tests the samples were pre-treated in oxygen/helium mixture ( $0.1 \text{ L min}^{-1}$ ) in the temperature range 298–798 K with a linear heating rate of  $2 \text{ K min}^{-1}$  and then for 1 h at 798 K. The standard test conditions were 1 h at 573–773 K with increasing reaction temperature every 50 K interval. The NO conversions were calculated from measured concentration of nitric oxide.

## 3. Results and discussion

### 3.1. Textural properties of $\text{V}_x\text{SiBEA}$

As shown in Fig. 1, the nitrogen adsorption/desorption isotherms of SiBEA and  $\text{V}_x\text{SiBEA}$  may be classified as type I according to IUPAC. All zeolite materials have similar BET surface area and micropore volume (Table 1) indicating that textural properties of BEA zeolite are preserved and there is no formation of mesoporosity upon dealumination of BEA zeolite and incorporation of vanadium atoms into SiBEA. Only  $\text{V}_{7.5}\text{SiBEA}$  has slightly lower specific surface area, probably due to the formation of vanadium oxide which block access to some pores and/or to the modification of density of the solid.

The XRD patterns of  $\text{V}_{1.0}\text{SiBEA}$  and  $\text{V}_{3.0}\text{SiBEA}$  are similar and no diffraction peaks due to crystalline phases other than BEA structure are observed suggesting, that vanadium ions are well dispersed in SiBEA matrix and two-steps preparation method does not affect

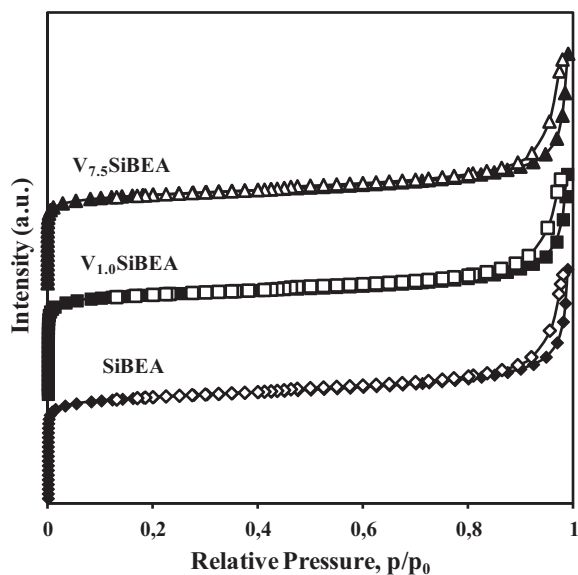


**Fig. 1.** Adsorption isotherms of nitrogen at 77 K of SiBEA, V<sub>1.0</sub>SiBEA and V<sub>7.5</sub>SiBEA samples. Full symbols: adsorption; empty symbols: desorption. For convenience, the dataset for V<sub>1.0</sub>SiBEA and V<sub>7.5</sub>SiBEA are shifted upwards along the Y-axis.

**Table 1**

Textural properties of TEABEA, AIBEAE, SiBEA and V<sub>x</sub>SiBEA zeolites.

Samples	Specific surface area $S_{\text{BET}}$ ( $\text{m}^2 \text{g}^{-1}$ )	Micropores volume $V_{\text{mic}}$ ( $\text{cm}^3 \text{g}^{-1}$ )
TEABEA <sup>a</sup>	59	0.03
AIBEAE <sup>b</sup>	605	0.23
SiBEA	661	0.26
V <sub>1.0</sub> SiBEA	652	0.28
V <sub>2.0</sub> SiBEA	652	0.25
V <sub>7.5</sub> SiBEA	575	0.23

<sup>a</sup> The parent tertaethylammonium BEA zeolite.

<sup>b</sup> TEABEA zeolite (Si/Al = 17) was calcined in static air at 823 K for 15 h.

zeolite crystalline structure [27,29]. Only for V<sub>7.5</sub>SiBEA (Fig. 2), additional diffraction peaks are observed in XRD profile attributed to vanadium compounds – V<sub>2</sub>O<sub>5</sub> (▼) and VO<sub>2</sub> (\*) in line with earlier report on high loading vanadium rutile [30,31].

Samples tested for SCR of NO reaction were also analyzed to investigate the stability of the prepared materials. As it is seen in Fig. 1, XRD pattern of spent-V<sub>1.0</sub>SiBEA is very similar to that of V<sub>1.0</sub>SiBEA, suggesting that upon SCR of NO reaction the structure of this catalyst is not changed. In contrast, the new XRD peaks of V<sub>2</sub>O<sub>5</sub> [30] are found for spent-V<sub>7.5</sub>SiBEA suggesting that sintering of vanadium oxide species takes place during reaction.

### 3.2. FTIR evidence of vanadium incorporation in the framework of SiBEA zeolite

The FTIR spectra of SiBEA and V<sub>1.0</sub>SiBEA are shown in Fig. 3. SiBEA, obtained by treatment of parent TEABEA zeolite with nitric acid solution exhibits three bands at 3735, 3705 and 3520  $\text{cm}^{-1}$ , ascribed to isolated internal, terminal internal and hydrogen bonded SiO–H located in vacant T-atom sites forming hydroxyl nest in agreement with earlier reports [24,25]. The impregnation of SiBEA zeolite with aqueous NH<sub>4</sub>VO<sub>3</sub> solution at pH 2.7 result in the decreasing of intensity of the broad band at 3520  $\text{cm}^{-1}$  due to the reaction of SiO–H groups with the mononuclear VO<sub>2</sub><sup>+</sup> ions. As a result, a new broad band at 3615  $\text{cm}^{-1}$  occurs in the spectrum of V<sub>1.0</sub>SiBEA attributed to the hydroxyl vibrator of V(V)O–H group, in line with earlier reports [32,33].

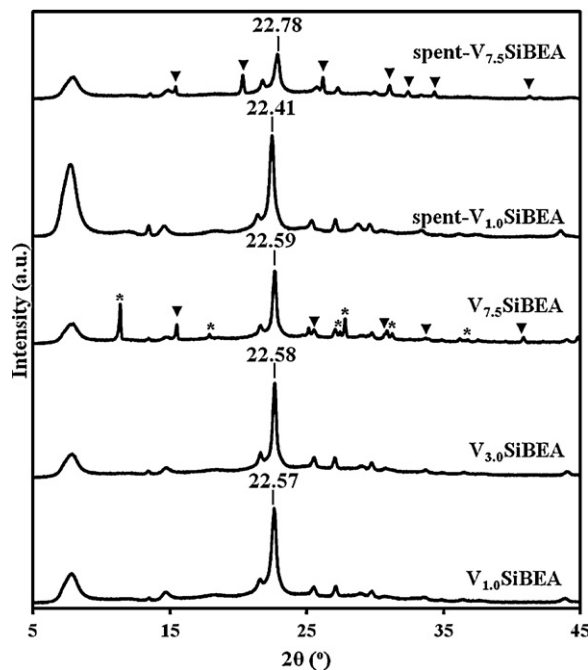


**Fig. 2.** X-ray diffractions of V<sub>1.0</sub>SiBEA, V<sub>3.0</sub>SiBEA, V<sub>7.5</sub>SiBEA, spent-V<sub>1.0</sub>SiBEA, and spent-V<sub>7.5</sub>SiBEA recorded at room temperature and ambient atmosphere (\* stand for VO<sub>2</sub> and ▼ for V<sub>2</sub>O<sub>5</sub>).

An additional evidence of vanadium incorporation into the zeolite framework is strong modification of IR band at 950  $\text{cm}^{-1}$  (Fig. 4) assigned to the stretching vibration of Si–O belonging to the uncoupled SiO<sub>4</sub> tetrahedra with a hydroxyl group, in line with earlier work on BEA zeolite [34–37]. After contacting SiBEA with the solution containing VO<sub>2</sub><sup>+</sup> ions, new bands at 975 and 945  $\text{cm}^{-1}$  appeared in FTIR spectrum of V<sub>1.0</sub>SiBEA, resulting from the incorporation of vanadium ions into vacant T-atom sites and

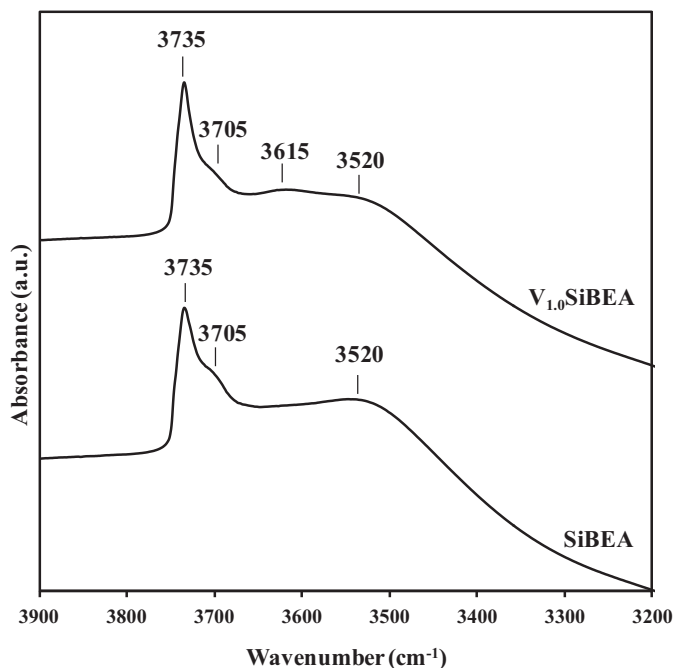
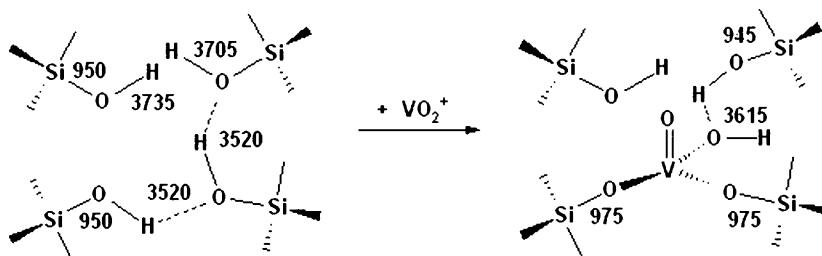


**Fig. 3.** FTIR spectra recorded at room temperature of SiBEA and V<sub>1.0</sub>SiBEA in the vibrational range of OH group.



**Scheme 1.** Schematic representation of hydroxyl nests (left) and framework pseudo-tetrahedral V(V) species. The number quoted corresponds to  $\text{cm}^{-1}$ .

the modification of the stretching vibrations of Si–O, as shown in Scheme 1.

### 3.3. Nature and environment of vanadium in $V_x\text{SiBEA}$

The DR UV–vis measurements are carried out to study the nature and environment of the vanadium in  $V_x\text{SiBEA}$ . The DR UV–vis spectrum of  $V_{1.0}\text{SiBEA}$  (Fig. 5) reveals two main bands at 265 and 340 nm attributed to oxygen-to-pseudo-tetrahedral V(V) charge transfer transition, involving oxygen in bridging V–O–Si and terminal V=O positions, respectively. In contrast, for  $V_{2.0}\text{SiBEA}$  the bands at 265 and 420 nm are attributed to oxygen-to-pseudo-tetrahedral V(V) and oxygen-to-octahedral V(V) charge transfer transition, respectively [38–41]. Additionally, in DR UV–vis spectrum of  $V_{7.5}\text{SiBEA}$  a new band at 485 nm appears corresponding to the presence of polynuclear V and/or vanadium oxide species [42].

Fig. 6 shows the Raman spectra of  $V_{1.0}\text{SiBEA}$  and  $V_{7.5}\text{SiBEA}$  recorded at ambient atmosphere. Both samples exhibit Raman bands related to zeolite framework and vibrational modes related to V species. Zeolite framework Raman features dominate the spectrum of the  $V_{1.0}\text{SiBEA}$  with low vanadium content (Fig. 6). Moreover, for  $V_{1.0}\text{SiBEA}$ , with low V content (1 wt.%), the Raman band at  $1040\text{ cm}^{-1}$  occurs assigned to V=O mode of mononuclear pseudo-tetrahedral V(V) species, in line with earlier report [43,44].

In contrast, for  $V_{7.5}\text{SiBEA}$ , with much higher V content (7.5 wt.%), the main Raman bands at  $991$ ,  $960$  and  $670\text{ cm}^{-1}$  occur due to the presence of polynuclear V species, in line with earlier reports [43–46]. These Raman results confirm DR UV–vis data presented in Fig. 5.

As shown in Fig. 7,  $V_{1.0}\text{SiBEA}$  reveals no EPR signal at 77 K indicating the absence of paramagnetic  $\text{V}^{\text{IV}}$  signal. In contrast, spent- $V_{1.0}\text{SiBEA}$  exhibits paramagnetic  $\text{V}^{\text{IV}}$  signal with narrow hyperfine structures and the  $g$ -factor and  $A$  values typical of a  $\text{V}^{\text{IV}}$  species in a distorted octahedral environment, very similar to that observed earlier for  $V_x\text{SiBEA}$  systems [27,47–49]. For  $V_{7.5}\text{SiBEA}$ , only a very broad asymmetric signal centered at  $g \approx 1.98$ – $1.96$  appears which can be related to polynuclear V(IV) species [50]. In contrast, spent- $V_{7.5}\text{SiBEA}$  exhibits two paramagnetic  $\text{V}^{\text{IV}}$  signals, a very broad rather anisotropic signal centered at  $g \approx 1.98$ – $1.96$  and a paramagnetic  $\text{V}^{\text{IV}}$  signal with narrow hyperfine structures and the  $g$ -factor and  $A$  values typical of a  $\text{V}^{\text{IV}}$  species in a distorted octahedral environment, similar to that appeared for  $V_{7.5}\text{SiBEA}$  (Fig. 7). It is important to mention here that in this condition of registration of EPR spectra of  $V_x\text{SiBEA}$  and spent- $V_{7.5}\text{SiBEA}$  only octahedral V(IV) species are detected.

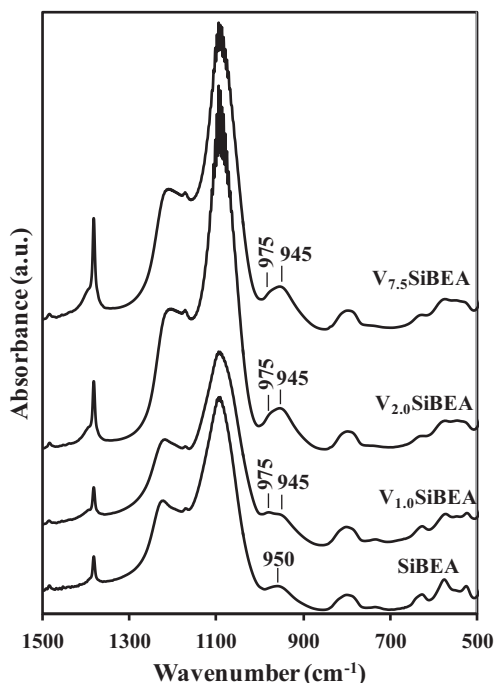


**Fig. 4.** KBr FTIR spectra recorded at ambient atmosphere of SiBEA,  $V_{1.0}\text{SiBEA}$ ,  $V_{2.0}\text{SiBEA}$  and  $V_{7.5}\text{SiBEA}$ .

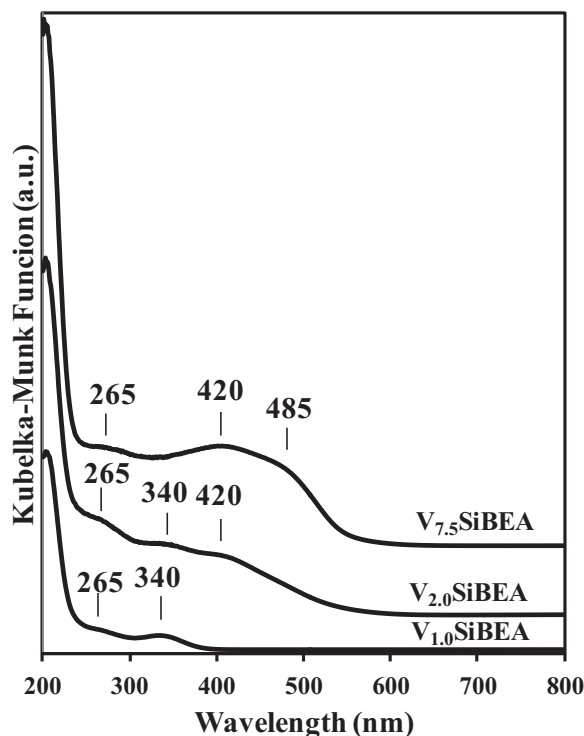


**Fig. 5.** DR UV–vis spectra recorded at ambient atmosphere of  $V_{1.0}\text{SiBEA}$ ,  $V_{2.0}\text{SiBEA}$  and  $V_{7.5}\text{SiBEA}$ .

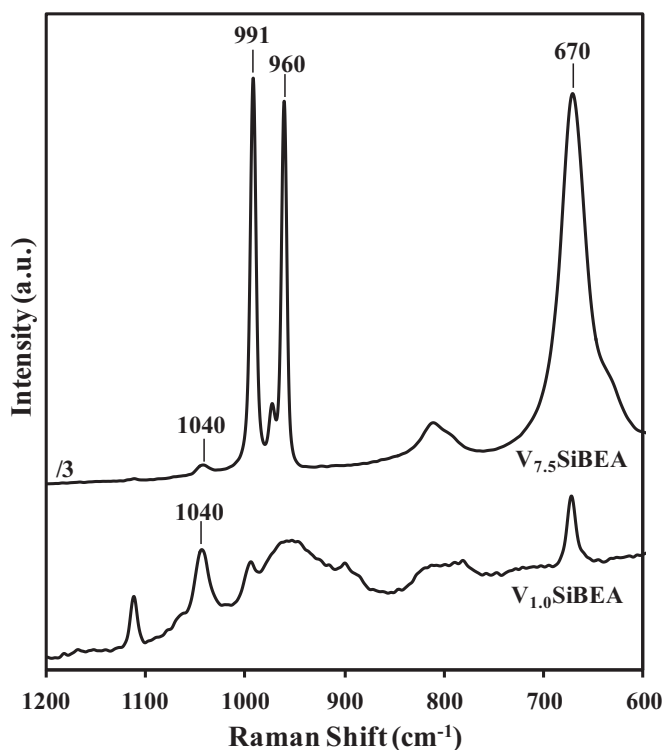


Fig. 6. Raman spectra of  $V_{1.0}\text{SiBEA}$  and  $V_{7.5}\text{SiBEA}$  recorded ambient atmosphere.

### 3.4. Reducibility of vanadium species

The  $\text{H}_2$ -TPR experiments were carried out on  $V_x\text{SiBEA}$  to investigate reducibility of vanadium species. As shown in Fig. 8, in TPR profile of  $V_{2.0}\text{SiBEA}$  only one broad peak appears at 905 K suggesting that one type of vanadium species is present in this material. In contrast, for  $V_{7.5}\text{SiBEA}$ , a broad peak at 815 K is observed with a shoulder at 905 K. The peaks at 905 K and 815 K may be attributed to isolated framework pseudo-tetrahedral V(V) and extra-framework octahedral V(V) species, respectively, in line with our earlier work on  $\text{VSiBEA}$  [47] and the studies on V-silicalite [39], V- $\text{SiO}_2$  and V-

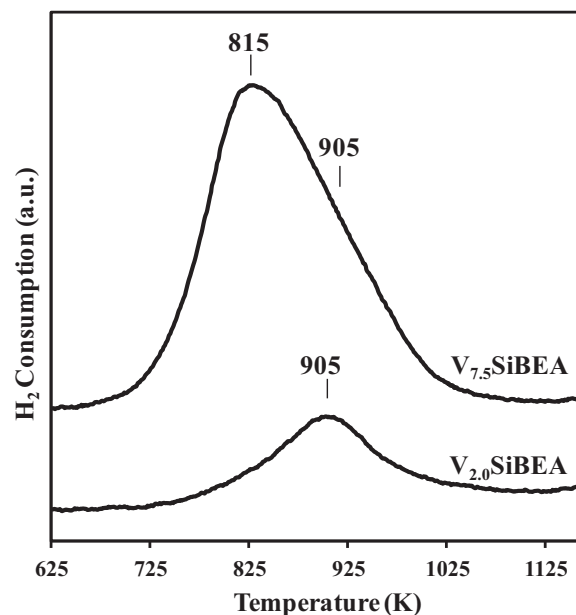
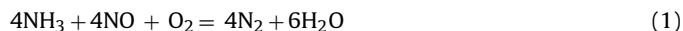


Fig. 8. TPR experiments of  $\text{H}_2$  consumption for  $V_{2.0}\text{SiBEA}$  and  $V_{7.5}\text{SiBEA}$ .

SBA-15 [51]. High hydrogen consumption at 815 K for  $V_{7.5}\text{SiBEA}$  suggests that mainly extra-framework octahedral V(V) species are present in this sample.

### 3.5. Catalytic activity of $V_x\text{SiBEA}$ zeolites

Selective catalytic reduction of NO with ammonia is based on the following reaction:



Generally, in the presence of transition metal containing catalyst the reaction proceeds rapidly in excess of oxygen and with ratio of  $\text{NO}/\text{NH}_3 = 1$  at temperature between 573 and 673 K. When temperature is increased to 723 K or higher, loss selectivity was observed and a competitive reaction of ammonia oxidation to  $\text{N}_2$ , NO and  $\text{N}_2\text{O}$  becomes important according to following reactions:



For vanadium catalyst the most common observed undesired product was nitrous oxides as reported earlier [12,25,52,53]. To avoid  $\text{N}_2\text{O}$  formation high dispersion of active species is required to hinder side reactions (2)–(4).

Catalytic performance – NO conversion and  $\text{N}_2\text{O}$  formation – is illustrated by Figs. 9 and 10, respectively. SiBEA support shows very low activity in SCR process with NO conversion lower than 15% in the whole temperature range. The introduction of vanadium into SiBEA framework lead to a huge increase of the NO conversion. As shown in Fig. 9, the NO conversion depends on both V content and the reaction temperature. For  $V_{1.0}\text{SiBEA}$ , containing mainly isolated pseudo-tetrahedral V(V) species conversion of NO increased with temperature and reached maximum of 60% at 773 K.

For  $V_{3.0}\text{SiBEA}$  catalyst, with the mixture of framework pseudo-tetrahedral and extra-framework octahedral V(V) species, (results not shown) a decrease in NO conversion in the high temperatures is observed. For the catalyst with high content of extra-framework octahedral V(V) species and vanadium oxide species a very sharp decrease in activity in SCR reaction at range 723–773 K is observed.

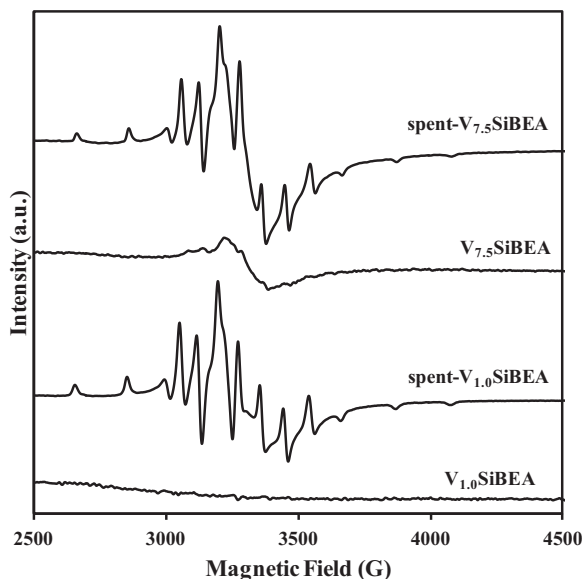
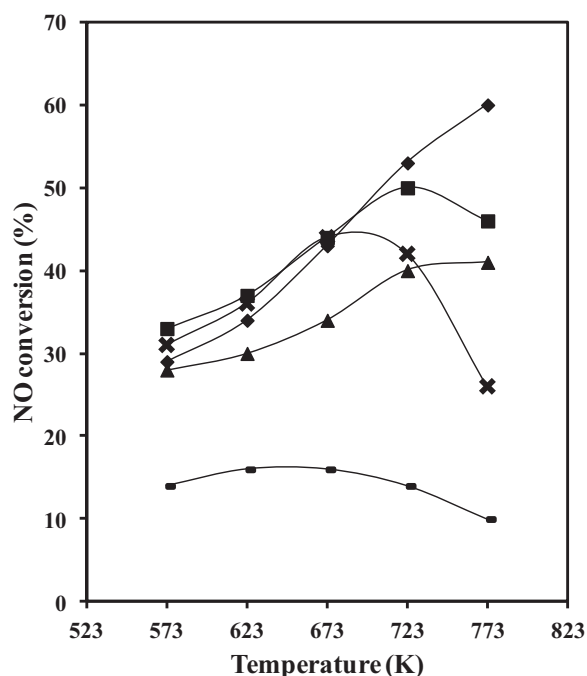
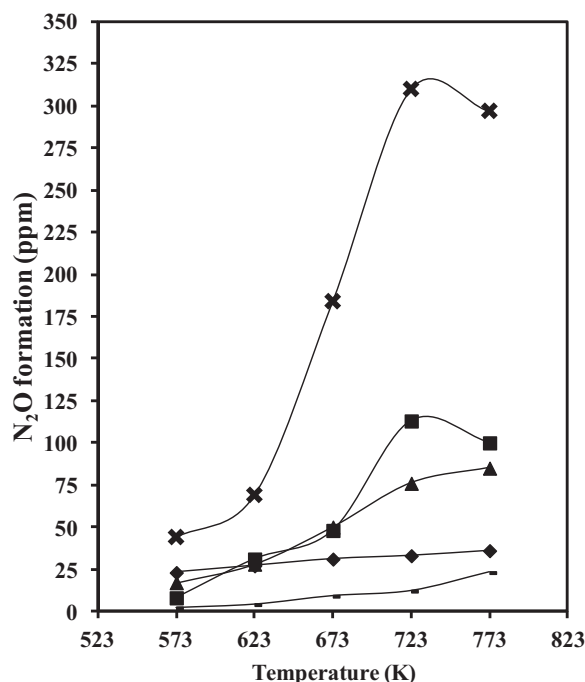


Fig. 7. EPR spectra of  $V_{1.0}\text{SiBEA}$ , spent- $V_{1.0}\text{SiBEA}$ ,  $V_{7.5}\text{SiBEA}$  and spent- $V_{7.5}\text{SiBEA}$  recorded at 77 K.



**Fig. 9.** Temperature-dependence of NO conversion in SCR of NO with ammonia on SiBEA (—■—), V<sub>1.0</sub>SiBEA (—◆—), V<sub>2.0</sub>SiBEA (—▲—), V<sub>3.0</sub>SiBEA (—■—) and V<sub>7.5</sub>SiBEA (—×—) catalysts.



**Fig. 10.** Temperature-dependence of N<sub>2</sub>O formation on SiBEA (—■—), V<sub>1.0</sub>SiBEA (—◆—), V<sub>2.0</sub>SiBEA (—▲—), V<sub>3.0</sub>SiBEA (—■—) and V<sub>7.5</sub>SiBEA (—×—) catalysts.

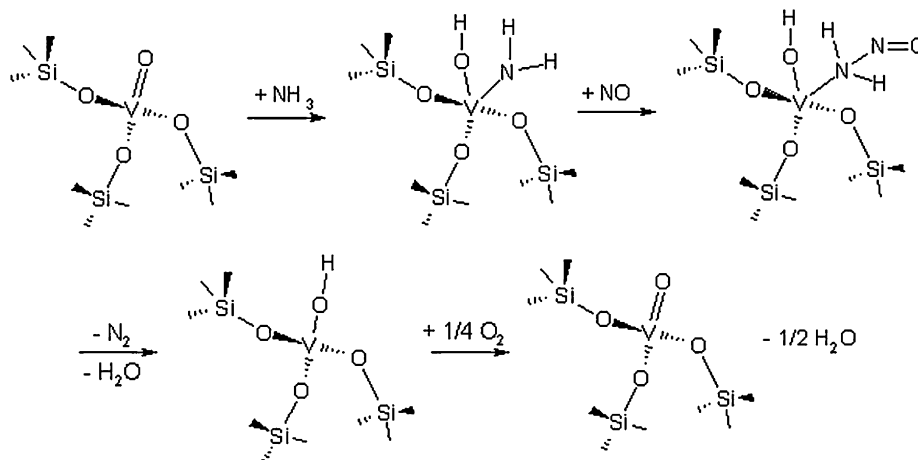
This is probably related to a competitive reaction of ammonia oxidation, as well as deactivation of catalysts due to the agglomeration of VO<sub>x</sub> species.

N<sub>2</sub>O formation is an indicator of SCR reaction selectivity. It generally increased with the increase of reaction temperature and vanadium content. For V<sub>7.5</sub>SiBEA catalyst containing vanadium oxides aggregates, as is evidenced by XRD, TPR and DR UV–vis, a sharp increase in the formation of N<sub>2</sub>O was observed. Taking into account that simultaneously the decrease of NO conversion occurs, it suggests that this by-product comes rather from NH<sub>3</sub> oxidation (reaction (4)) than SCR process itself.

On the other hand, the application of V<sub>1.0</sub>SiBEA containing mainly pseudo-tetrahedral V(V) species lead to a very low formation of N<sub>2</sub>O (around the accuracy limit of NDIR analyzer). Thus, it may be concluded that the presence of mononuclear framework vanadium sites has a very positive effect on SCR of NO with ammonia into N<sub>2</sub> (reaction (1)).

In contrast, polynuclear V species are much more active in oxidation of NH<sub>3</sub> by gaseous oxygen (reactions (2)–(4)), in line with earlier works [17,25,54]. However, our results suggest that at high temperature range polynuclear species are much less stable than mononuclear ones and very poor selectivity to a desired product is observed. The V<sub>x</sub>SiBEA catalysts, containing isolated pseudo-tetrahedral V(V) species have not only very high selectivity to desired product (N<sub>2</sub>) but also give high NO conversion at 773 K.

Several different mechanism pathways are proposed for SCR of NO with ammonia on vanadium-containing catalysts but no unequivocal conclusions are drawn. The present work and DFT theoretical investigations on V<sub>x</sub>SiBEA zeolites [43,55–58] seem to suggest that the most probable active sites in SCR of NO with ammonia are non-hydroxylated (SiO)<sub>3</sub>V(V)=O and/or hydroxylated (SiO)<sub>2</sub>(HO)V(V)=O vanadium species. The probable reaction pathway of SCR of NO with ammonia on non-hydroxylated (SiO)<sub>3</sub>V(V)=O center is proposed in Scheme 2. In the first step, ammonia adsorbs on non-hydroxylated (SiO)<sub>3</sub>V(V)=O center



**Scheme 2.** Probable pathway of SCR reaction with ammonia over framework pseudo-tetrahedral non-hydroxylated (SiO)<sub>3</sub>V(V)=O center.

resulting in the formation of  $(\text{SiO})_3\text{V(IV)}(\text{OH})\text{NH}_2$  intermediates. Then, nitric oxide is adsorbed, forming nitrosamine which is then decompose to  $\text{N}_2$  and  $\text{H}_2\text{O}$ . Finally,  $(\text{SiO})_3\text{V(IV)}\text{—OH}$  center is easily oxidized to  $(\text{SiO})_3\text{V(V)}=\text{O}$  ones by gaseous oxygen (Scheme 2).

#### 4. Conclusion

The procedure of catalysts preparation has significant influence on the nature and environment of V(V) species in  $\text{V}_x\text{SiBEA}$  zeolites, as evidenced by XRD, FTIR and DR UV–vis. For low V content (<2 V wt.%), the two-steps postsynthesis method allows to incorporate of  $\text{VO}_2^+$  ions into framework of SiBEA zeolite as isolated pseudo-tetrahedral V(V) species. In contrast, for higher V content, besides the isolated pseudo-tetrahedral V(V) species, the extra-framework octahedral V(V) and also vanadium oxide species are formed.

$\text{V}_{1.0}\text{SiBEA}$  catalyst with pseudo-tetrahedral vanadium species is active in SCR of NO by ammonia with the maximum conversion of 60% at 773 K and very low concentration of  $\text{N}_2\text{O}$  in the product stream. This catalytic properties of  $\text{V}_{1.0}\text{SiBEA}$  are related to a very high dispersion of vanadium in framework of zeolite as mononuclear pseudo-tetrahedral V(V) species.

The formation of  $\text{N}_2\text{O}$  increases with V content due to the presence in  $\text{V}_x\text{SiBEA}$  of extra-framework octahedral V(V) and/or vanadium oxide which promote rather ammonia oxidation than NO reduction, in particular, at the higher temperature range.

#### References

- [1] L. Lietti, I. Nova, G. Ramis, L. Dall'Acqua, G. Busca, E. Giamello, P. Forzatti, F. Bregani, *Journal of Catalysis* 187 (1999) 419–435.
- [2] L. Casagrande, L. Lietti, I. Nova, P. Forzatti, A. Baiker, *Applied Catalysis B* 22 (1999) 63–77.
- [3] M. Koebel, M. Elsener, *Chemical Engineering Science* 53 (1998) 657–669.
- [4] M.L. Moura de Oliveira, C. Monteiro Silva, R. Moreno-Tost, T. Lopes Farias, A. Jimenez-Lopez, E. Rodriguez-Castellon, *Applied Catalysis B* 88 (2009) 420–429.
- [5] S.S.R. Putluru, A. Riisager, R. Fehrmann, *Applied Catalysis B* 101 (2011) 183–188.
- [6] J. Li, H. Chang, L. Ma, J. Hao, R.T. Yang, *Catalysis Today* 175 (2011) 147–156.
- [7] U. De La Torre, B. Pereda-Ayo, J.R. González-Velasco, *Chemical Engineering Journal* 207–208 (2012) 10–17.
- [8] J. Janas, T. Machej, J. Gurgul, R.P. Socha, M. Che, S. Dzwigaj, *Applied Catalysis B* 75 (2007) 239–248.
- [9] A. Corma, V. Fornes, E. Palomares, *Applied Catalysis B* 11 (1997) 233–242.
- [10] D.W. Fickel, E. D'Addio, J.A. Lauterbach, R.F. Lobo, *Applied Catalysis B* 102 (2011) 441–448.
- [11] M. Anstrom, N.-Y. Topsøe, J.A. Dumesic, *Journal of Catalysis* 213 (2003) 115–125.
- [12] S.M. Jung, P. Grange, *Applied Catalysis B* 36 (2002) 325–332.
- [13] M. Koebel, G. Madia, F. Raimondi, A. Wokaun, *Journal of Catalysis* 209 (2002) 159–165.
- [14] Y.-K. Park, J.W. Lee, C.W. Lee, S.-E. Park, *Journal of Molecular Catalysis A* 158 (2000) 173–179.
- [15] M. Anstrom, N.-Y. Topsøe, J.A. Dumesic, *Catalysis Letters* 78 (2002) 281–289.
- [16] R.C. Adams, L. Xu, K. Moller, T. Bein, W.N. Delgass, *Catalysis Today* 33 (1997) 263–278.
- [17] S.S.R. Putluru, A. Riisager, R. Fehrmann, *Applied Catalysis B* 97 (2010) 333–339.
- [18] A. Lavata, C.E. Quinocesb, M.G. Gonzalez, *Materials Letters* 59 (2005) 2986–2989.
- [19] M. Mhamdi, A. Ghorbel, G. Delahay, *Catalysis Today* 142 (2009) 239–244.
- [20] M. Wark, A. Bruckner, T. Liese, W. Grunert, *Journal of Catalysis* 175 (1998) 48–61.
- [21] G. Piehl, T. Liese, W. Grunert, *Catalysis Today* 54 (1999) 401–406.
- [22] D. Worch, W. Suprun, R. Glaser, *Catalysis Today* 176 (2011) 309–313.
- [23] T. Fushun, Z. Ke, Y. Fang, Y.G. Lili, X. Bolian, Q. Jinheng, F. Yining, *Chinese Journal of Catalysis* 33 (2012) 933–940.
- [24] G. Madia, M. Elsener, M. Koebel, F. Raimondi, A. Wokaun, *Applied Catalysis B* 39 (2002) 181–190.
- [25] P. Forzatti, *Applied Catalysis A* 222 (2001) 221–236.
- [26] R.M. Caraba, S.G. Masters, K.M. Eriksen, V.I. Parvulescu, R. Fehrmann, *Applied Catalysis B* 34 (2001) 191–200.
- [27] R. Baran, Y. Millot, T. Onfroy, F. Averseng, J.-M. Krafft, S. Dzwigaj, *Microporous and Mesoporous Materials* 161 (2012) 179–186.
- [28] C.F. Baes Jr., R.E. Mesmer, *The Hydrolysis of Cations*, Krieger Publishing Company, Malabar, 1986, Reprint edition, p. 210.
- [29] M. Trejda, M. Ziolek, Y. Millot, K. Chalupka, M. Che, S. Dzwigaj, *Journal of Catalysis* 281 (2011) 169–176.
- [30] L.F. Borisenko, E.K. Serafimova, M.E. Kazakova, N.G. Shumyatskaia, *Doklady Akademii Nauk SSSR* 193 (1970) 683–686.
- [31] B. Schimmoller, R. Delaigle, D.P. Debecker, E.M. Gaigneaux, *Catalysis Today* 157 (2010) 198–203.
- [32] R. Hajjar, Y. Millot, P.P. Man, M. Che, S. Dzwigaj, *Journal of Physical Chemistry C* 112 (2008) 20167–20175.
- [33] F. Tielens, M. Calatayud, S. Dzwigaj, M. Che, *Microporous and Mesoporous Materials* 119 (2009) 137–147.
- [34] Q.-H. Xia, S.-C. Shen, J. Song, S. Kawi, K. Hidajat, *Journal of Catalysis* 219 (2003) 74–84.
- [35] C. Yang, Q. Xu, *Zeolites* 19 (1997) 404–410.
- [36] C. Yang, Q. Xu, C. Hu, *Materials Chemistry and Physics* 63 (2000) 55–66.
- [37] R. Dimitrova, G. Gunduz, L. Dimitrov, T. Tsoncheva, S. Yalmaz, E.A. Urqueta-Gonzalez, *Journal of Molecular Catalysis A* 214 (2004) 265–268.
- [38] S. Dzwigaj, P. Massiani, A. Davidson, M. Che, *Journal of Molecular Catalysis* 155 (2000) 169–182.
- [39] G. Centi, S. Perathoner, F. Trifiro, A. Aboukais, C.F. Adssi, M. Guelton, *Journal of Physical Chemistry* 96 (1992) 2617–2629.
- [40] M.K. de Pietre, F.A. Bonk, C. Rettori, F.A. Garcia, H.O. Pastore, *Microporous and Mesoporous Materials* 145 (2011) 108–117.
- [41] M. Piumetti, B. Bonelli, P. Massiani, Y. Millot, S. Dzwigaj, L. Gaberova, M. Armandi, E. Garrone, *Microporous and Mesoporous Materials* 142 (2011) 45–54.
- [42] Y.-M. Liu, Y. Cao, N. Yi, W.-L. Feng, W.-L. Dai, S.-R. Yan, H.-Y. He, K.-N. Fan, *Journal of Catalysis* 224 (2004) 417–428.
- [43] A.E. Lewandowska, M.A. Banares, F. Tielens, M. Che, S. Dzwigaj, *Journal of Physical Chemistry C* 114 (2010) 19771–19776.
- [44] D.E. Keller, T. Visser, F. Soulimani, D.C. Koningsberger, B.M. Weckhuysen, *Vibrational Spectroscopy* 43 (2007) 140–151.
- [45] M. Piumetti, B. Bonelli, P. Massiani, S. Dzwigaj, I. Rossetti, S. Casale, L. Gaberova, M. Armandia, E. Garrone, *Catalysis Today* 176 (2011) 458–464.
- [46] C. Hess, J.D. Hoefelmeyer, T. Don Tilley, *Journal of Physical Chemistry* 108 (2004) 9703–9709.
- [47] S. Dzwigaj, E.M. El Malki, M.-J. Peltre, P. Massiani, A. Davidson, M. Che, *Topics in Catalysis* 11/12 (2000) 379–390.
- [48] S. Dzwigaj, M. Che, *Journal of Physical Chemistry B* 109 (2005) 22167–22174.
- [49] P. Pietrzyk, Z. Sojka, S. Dzwigaj, M. Che, *Journal of the American Chemical Society* 129 (2007) 14174–14175.
- [50] Z. Luan, L. Kevan, *Journal of Physical Chemistry B* 101 (1997) 2020–2027.
- [51] M. Piumetti, B. Bonelli, P. Massiani, S. Dzwigaj, I. Rossetti, S. Casale, M. Armandia, C. Thomas, E. Garrone, *Catalysis Today* 179 (2012) 140–148.
- [52] N.-Y. Topsøe, H. Topsøe, J.A. Dumesic, *Journal of Catalysis* 151 (1995) 226–240.
- [53] S. Suárez, S.M. Jung, P. Avila, P. Grange, J. Blanco, *Catalysis Today* 75 (2002) 331–338.
- [54] L. Lietti, P. Forzatti, *Journal of Catalysis* 147 (1994) 241–249.
- [55] A. Wojtaszek, M. Ziolek, S. Dzwigaj, F. Tielens, *Chemical Physics Letters* 514 (2011) 70–73.
- [56] F. Tielens, S. Dzwigaj, *Chemical Physics Letters* 501 (2010) 59–63.
- [57] F. Tielens, S. Dzwigaj, *Catalysis Today* 152 (2010) 66–69.
- [58] S. Dzwigaj, M. Matsuoka, M. Anpo, M. Che, *Journal of Physical Chemistry B* 104 (2000) 6012–6020.